JOURNAL OF GEOPHYSICAL RESEARCH, VOL. 102, NO. D15, PAGES 19,137–19,148, AUGUST 20, 1997

A UARS study of lower stratospheric polar processing in the early stages of northern and southern winters

V. A. Yudin,[1,2] M. A. Geller,[1] B. V. Khattatov,[1] A. R. Douglass,[3] M. C. Cerniglia,[3] J. W. Waters,[4] L. S. Elson,[4] A. E. Roche,[5] and J. M. Russell III[6]

Abstract. UARS data and results from a three-dimensional transport model have been used to compare and contrast the extent of the early stages of chemical processing by polar stratospheric clouds (PSCs) during the 1991–1993 northern and southern hemisphere winters of the Upper Atmosphere Research Satellite (UARS) mission. The modeled location and timing of regions of polar processing agree quite well with the UARS microwave limb sounder (MLS), cryogenic limb array etalon spectrometer (CLAES) and Halogen Occultation Experiment (HALOE) observations in that enhanced ClO concentrations are generally found in sunlit regions of polar-processed air and decreases of $ClONO_2$ and HNO_3 accompany low temperatures and high values of the aerosol extinctions inside the vortex. For these winters it is found that there is a period of about 2 weeks during the northern hemisphere early winter where sporadic polar processing takes place. After this a persistent processing region is seen inside the polar vortex, and the vortex fills with polar-processed air in a bit more than 2 weeks from the first persistent PSC occurrence. In the southern hemisphere, polar processing also fills the vortex in a bit over 2 weeks. Estimates of the spectral aerosol measure of the aerosol spectrum from CLAES observations illustrate that PSC particles are seen where cold temperatures occur inside the polar vortex and heterogeneous conversion of chlorine species on PSCs are expected.

1. Introduction

Prior to the discovery of the Antarctic ozone hole by *Farman et al.* [1985], the paradigm for understanding the distribution of stratospheric ozone involved gas phase photochemistry and transport. This concept has now fundamentally changed, and the great importance of heterogeneous chemical reactions in determining the ozone distribution in both polar regions [e.g., *Solomon*, 1990; *Tuck et al.*, 1992] and at midlatitudes [e.g., *Rodriguez et al.*, 1991] is now generally appreciated. In this paper we expand on previous studies by *Douglass et al.* [1993] and *Geller et al.* [1993, 1995] in using winds and temperatures from the Goddard Earth Observing System–Data Assimilation System (GEOS-DAS) together with a transport model to study the heterogeneous conversion of chlorine constituents on polar stratospheric cloud (PSC) particles in the lower stratosphere (hereinafter referred to as "polar processing"). In particular, we use this model to guide us in studying Upper Atmosphere Research Satellite (UARS) data on ClO, HCl, $ClONO_2$, and aerosols to enhance our understanding of the similarities and differences between early winter polar processing in the northern and southern hemispheres. We examine the two northern hemisphere (NH) winters 1991–1992 and 1992–1993 and two southern hemisphere (SH) winters 1992 and 1993. For this study, the transport model serves as a guide to the geographical extent and evolution of polar processing during the early stages of these winters. We will compare and discuss the results of the modeled polar processing, with observations of temperature, chemical constituents, and aerosols from the microwave limb sounder (MLS), cryogenic limb array etalon spectrometer (CLAES) and Halogen Occultation Experiment (HALOE) instruments, all on UARS. The objectives of the study are (1) to compare the main features of polar processing in the northern and southern polar regions, (2) to see how the polar processing evolves during the winter, and (3) to further assess the consistency of the transport model with UARS observations.

Several recent papers have dealt with three-dimensional (3-D) simulations of polar processing during some of these winters. *Chipperfield et al.* [1994] looked at chlorine activation and PSC processing during the Arctic winter 1991–1992. *Chipperfield* [1994] discussed PSC processing during the Arctic winters of 1991–1992 and 1992–1993. These studies focused mainly on how the different evolution of these two NH winters led to different possibilities for the ozone depletion, especially during the later stages of these winters. *Lefevre et al.* [1994] completed full chemistry simulations for the NH 1991–1992 winter. They emphasized the role played by the Mount Pinatubo stratospheric aerosols in producing enhanced ClO concentrations at middle and high latitudes. They also pointed out their good agreement with aircraft and UARS/MLS observations of chlorine monoxide [*Toohey et al.*, 1993; *Waters et al.*, 1993a].

In this work we examine the evolution of polar processing

[1]Institute for Terrestrial and Planetary Atmospheres, State University of New York at Stony Brook.
[2]On leave from Meteorology Department, Russian Institute for Hydrology and Meteorology, St. Petersburg.
[3]Laboratory for Atmospheres, NASA Goddard Space Flight Center, Greenbelt, Maryland.
[4]Jet Propulsion Laboratory, California Institute of Technology, Pasadena.
[5]Lockheed Palo Alto Research Laboratory, Palo Alto, California.
[6]NASA Langley Research Center, Hampton, Virginia.

Paper number 97JD00871.
0148-0227/97/97JD-00871$09.00

during early winter from initiation to the point where the polar-processed air fills the polar vortex. The combined analysis of transport calculations and UARS data from different instruments provides an opportunity to discuss the main features of the polar processing and the contrasts between the Arctic and Antarctic winter situations.

In the following sections we explain our modeling procedures, describe the UARS data sources, show and discuss our transport results together with UARS data and compare our results with those of previous studies.

2. Modeling Procedures

Our modeling strategy is based on the simple transport calculations of *Douglass et al.* [1991, 1993] and *Kaye et al.* [1991]. Depletions of the "quasi-conservative" constituent HCl are used as indicators for polar processing in the same manner as in these works. The idea of using HCl is to study the behavior of one of the key heterogeneous reactions in which chlorine compounds are transformed from reservoir to active forms on the surfaces of PSCs:

$$HCl(s) + ClONO_2(g) \rightarrow HNO_3(s) + Cl_2(g) \qquad (1)$$

Here the symbols (s) and (g) denote solid and gas phase states. The same reaction takes place also on the surfaces of sulfate aerosols, although at a much slower rate at typical middle latitude lower stratospheric temperatures:

$$HCl(a) + ClONO_2(g) \rightarrow HNO_3(g) + Cl_2(g) \qquad (2)$$

Here "(a)" denotes aerosol particles. The reactive chlorine species that are responsible for the catalysis of ozone loss are formed through photolysis of Cl_2 and the subsequent reaction of Cl with O_3 [*Solomon*, 1990]. In particular, ClO as a reactive compound is formed under sunlit conditions. In this and previous papers, the measure of the heterogeneous polar processing on PSCs due to reaction (1) is denoted by DHCl (depleted HCl). DHCl is defined as the difference between the HCl concentrations that would exist in the absence of heterogeneous reaction (1) and that computed with (1) occurring on PSCs. DHCl in the transport simulations is a crude indicator of the degree to which inactive chlorine species have been converted into reactive chlorine. It is not ClO, nor is it proportional to ClO. The amount of ClO produced in polar processed air by (1) and other heterogeneous reactions on PSCs and sulfate aerosols [see *Danilin and McConnell*, 1994] depends on the exposure of processed air to sunlight and the photochemical partitioning of the odd chlorine family. The calculated distribution of DHCl gives us information about the predicted location of the products of (1) and shows areas of predicted heterogeneous losses of HCl and $ClONO_2$.

We use the NASA Goddard 3-D transport model in which the winds and temperatures are derived from the GEOS-DAS troposphere-stratosphere data assimilation system [*Schubert et al.*, 1993]. This model and its modification have been described in several previous papers [e.g., *Cerniglia et al.*, 1995; *Allen et al.*, 1991]. We initialize the 3-D HCl distribution using the method of *Lary et al.* [1995] to map the HCl distribution taken from the two-dimensional model of *Smyshlyaev and Yudin* [1995] into potential vorticity (PV)–potential temperature (PT) coordinates. Two three-dimensional "HCl" distributions are generated by this transport model. One is obtained using the gas phase production and loss rates from *Smyshlyaev and Yudin* [1995] and the other uses an additional HCl loss rate with a 0.5-day e-folding time when the temperature T falls below a critical value given by T_c, where T_c represents the threshold temperature for type I PSC (PSC I) formation. The values for T_c are taken from the expressions by *Hanson and Mauersberger* [1988], which describe the thermodynamic conditions for the formation of nitric acid trihydrate (NAT). The temperature threshold used in our transport experiments is 2°K warmer than the threshold given by *Hanson and Mauersberger* [1988]. The use of this warmer critical temperature value is motivated by the study of *Schoeberl et al.* [1993a, b] in which back trajectories were calculated using National Meteorological Center (NMC) analyses for locations along aircraft flight tracks. Their results showed that almost all of the parcels that encountered NMC temperatures within 3°K of the NAT temperatures from *Hanson and Mauersberger* [1988] showed elevated ClO concentrations, implying that they had experienced polar processing. We take DHCl to indicate the degree of polar processing an air parcel has experienced.

Because ClO_x should be in its dimer form Cl_2O_2 in the absence of sunlight, we expect to observe ClO enhancement only when polar-processed air is in sunlight, although the enhancement of ClO can also decrease in sunlit regions due to other chemical reactions, for instance chlorine nitrate formation through reaction of ClO with NO_2. Finally, we emphasize that for high concentrations of volcanic aerosol, as observed for the 1991–1992 Arctic and 1992 Antarctic winters, reaction (2) and as well as other heterogeneous reactions may take place at (and below) the relatively warm temperature of 210°K (see, for example, *Murphy and Ravishankara* [1994] and *Hanson et al.* [1994]). Thus the key difference between products of HNO_3 due to reactions (1) and (2) is that HNO_3 produced by (1) remains on the PSC surface until the cloud evaporates, while reaction (2) on sulfate aerosols enhances gas phase concentrations of nitric acid. Both reactions give heterogeneous losses of HCl and $ClONO_2$.

3. UARS Data

Given that the transport model uses temperatures and winds from the GEOS-DAS analyses, we can compare daily sequences from our model simulation with UARS measurements. Thus we can see whether UARS measurements show reasonable agreement with our transport calculations of the polar heterogeneous processing due to reaction (1) on PSCs. Qualitative agreement between model results and UARS observations gives confidence in our ability to use model results to fill in those parts of the time-space domain for which UARS measurements are unavailable owing to the spacecraft viewing geometry [*Reber*, 1993]. In this paper we use data from the MLS, CLAES, and HALOE instruments on UARS [*Barath et al.*, 1993; *Roche et al.*, 1993a; *Russell et al.*, 1993]. The UARS spacecraft flies at an inclination of 57° and an altitude of about 585 km. Thus the spacecraft orbit precesses in local time, and the latitude that separates daytime viewing from nighttime viewing changes with time. This is important for MLS ClO viewing because significant concentrations of ClO are expected to be present only under sunlit conditions. Also, the precessing orbit of UARS makes it necessary that the spacecraft execute a yaw maneuver approximately every 40 days to ensure that the same side of the spacecraft always faces away from the Sun [*Reber*, 1993]. This implies that the high latitudes of each hemisphere are viewed by MLS and CLAES for alternating yaw

periods. For instance, when the cold side of UARS faces north, MLS and CLAES obtain data from about 33°S to 80°N. The systematic and random errors for CLAES data, discussed in this paper, are 20% and 1 ppbv for the HNO_3 volume-mixing ratio (VMR), and 30% and 0.3 ppbv for $ClONO_2$ [*Roche et al.*, 1993b, 1994]. The CLAES team [*Roche et al.*, 1994] also estimates a systematic error in most of the aerosol extinction data used in this paper to be 20% with a repeatability of 15% in the lower stratosphere. The CLAES temperatures have systematic errors between 2° and 4°K [*Roche et al.*, 1994]. MLS data validation indicates individual measurement accuracies of ~0.4 ppbv for 46-hPa ClO [*Waters et al.*, 1996]. The HALOE errors in retrieved HCl profiles are approximately 5% (random) and 15% (systematic) [*Russell et al.*, 1993]. Version 3 MLS, version 7 CLAES, and version 16 HALOE data are used in this paper.

4. Model and Data Analysis Periods

In this paper we concentrate on the periods from the initiation of polar processing to the time when the polar vortex is filled with chemically processed air. We analyze the first two northern and southern hemisphere polar-processing periods for which there are UARS observations, to examine the differences between the development of polar processing in the northern and southern hemispheres. No attempt is made to simulate the full chemistry of the polar regions as was attempted by *Lefevre et al.* [1994], for example. In this paper we focus on the early part of the 1991–1992 NH winter and the 1992 SH winter, when we have the CLAES observations of $ClONO_2$, HNO_3, and aerosols, and analyze the consistency of the high-latitude HALOE measurements of HCl with CLAES and MLS observations for the NH winter 1991–1992. A comparison with the next two UARS winters is also considered briefly. Figure 1 summarizes the evolution of the cold polar areas during the NH and SH winters 1991–1993 on the basis of the minimum temperature north of 40°N (top two rows) and south of 40°S (bottom two rows) in the GEOS-DAS analysis from December 1 to January 30 in the NH and from May 1 to July 30 in the SH at 46 hPa. The periods when MLS and CLAES observed the polar regions are between the shaded bars at the bottom of each panel. The first column of Figure 1 shows that in the early stages of SH winters we expect to see quasi-monotonic (continuous) filling of the polar vortex with air that is chemically processed on PSC particles. During the first 2 weeks of the NH winters (top two rows of Figure 1), the minimum temperatures oscillate around the NAT temperature threshold (195°K), and as pointed out by *Douglass et al.* [1993], sporadic polar-processing events take place before the permanent filling of the northern vortex by chemically perturbed air. More detailed analysis of the basic features of polar processing during the early stages of these UARS winters are presented in the next section.

5. Results

In this section, the results for the temperature, potential vorticity, and DHCl from the assimilation and transport models are shown and compared with UARS observations of HCl, ClO, $ClONO_2$, HNO_3, and aerosol distributions.

5.1. Northern Hemisphere Winters 1991–1992 and 1992–1993

The GEOS-DAS temperature fields and modeled DHCl for 1200 UT on the 465°K PT surfaces are shown in the top row of Plate 1 for December 7 and 13 and January 10. These days have been selected to illustrate three stages of polar processing in the NH winter 1991–1992. December 7 is a day shortly after the first occurrence of polar processing, December 13 is a day when filling of the vortex is progressing, and January 10 is a day when the polar vortex is completely filled with chemically processed air. In this figure the north pole is at the center of each plot and the outer edge is at 30°N. The 60°N and 80°N latitude circles are also shown. The contour within which the temperature is less than 195°K is outlined in black. The white lines are approximate polar vortex boundaries with PV values of 2.8 and 3.1×10^{-5} °K m^2 s^{-1} kg^{-1}. As the winter evolves we can follow the filling of the polar vortex with processed air by referring to these contours. The white circles on the DHCl maps show the boundary between MLS nighttime measurements (to the north) and daytime measurements (to the south). The first sign of polar processing in our model is found on December 5 at about 80°N, 0°E, when the first temperatures less than 197°K are seen at about 75°N (Figure 1) at a longitude of about 45°W. Two days later, on December 7 (Plate 1), the region of polar processing, as seen in terms of DHCl, has been transported equatorward and enlarged through shearing so that it now lies at about 60°N, 60°E, in the region of MLS sunlit observations. On December 13 there are two broader DHCl regions displaying the progression of polar processing. By December 29, as shown by our DHCl calculations (but not shown in Plate 1) the polar vortex is filled with polar-processed air (DHCl). Thus after this date, deformations in the polar vortex define the region of polar-processed air. For instance, on January 10, a few days before a strong warming takes place, we see a strong displacement of the vortex toward 45°E. The areas of coldest air have expanded and shifted southward, and the vortex is filled with highly processed air (high values of DHCl).

The last row of Plate 1 shows MLS daytime observations of ClO at a pressure level of 46 hPa (a pressure altitude lying very near the PT altitude of 465°K). To generate these maps, we have plotted daytime ClO measurements (defined as having the measurement solar zenith angle less than 94°) for each day. We used level 3AT MLS CLO data and asynoptic mapping procedures described by *Elson and Froidevaux* [1993]. In each of these plots, the white circle in the polar region shows the area within which there exist only nighttime ClO measurements. Within this circle, the dimer Cl_2O_2 is the dominant ClO_x species. As was mentioned above, owing to the precession of the UARS orbit, this MLS nighttime region varies with each measurement day. The quoted rms precision of 46-hPa MLS ClO measurements is 0.4 ppbv [*Waters et al.*, 1996], so we focus on ClO concentrations greater than this. On December 5, as is shown by the MLS ClO maps, no significant patches of ClO are seen around the vortex boundaries, consistent with the fact that polar-processed air was seen only in regions of MLS nighttime observations. Isolated larger values of ClO can also occur as a result of instrument noise, and *Schoeberl et al.* [1993b] have shown that these isolated values outside the 1991–1992 polar winter vortex are consistent with the expected noise distribution. On December 7, high concentrations of ClO are seen at about 50°–60°N, 40°–50°E. This is slightly to the east of the high values of DHCl in Plate 1 on this day. Given the inexactness of the mapping procedure used for ClO, this is a reasonable coincidence and confirms that we have followed the transport of the first polar-processing event during the early stages of the NH winter 1991–1992. On December 13, several regions of large concentrations of ClO are seen by

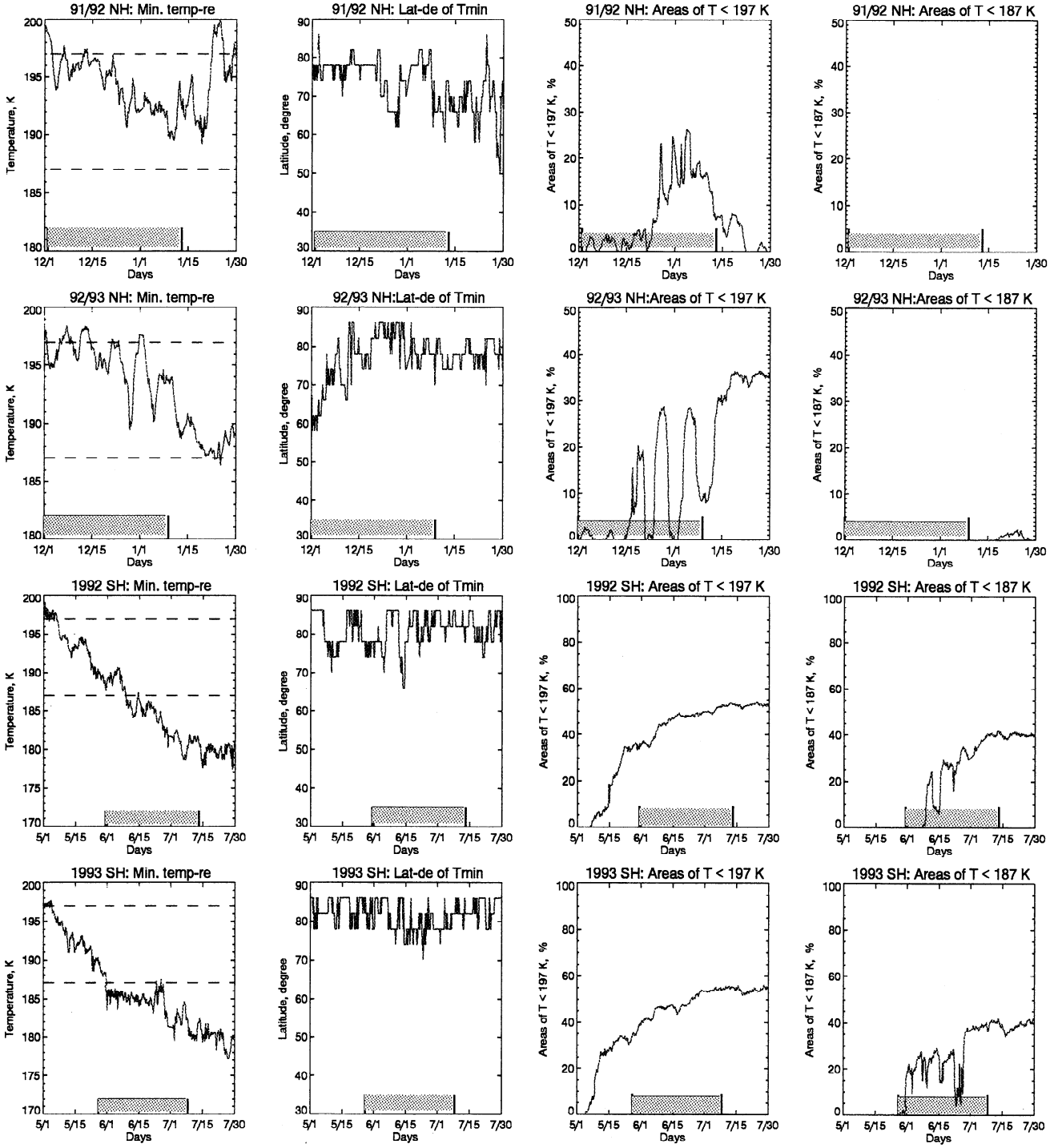

Figure 1. GEOS-DAS picture of the cold air evolution on the 46-hPa pressure surface in the (top to bottom) 1991–1992 Arctic, 1992–1993 Arctic, 1992 Antarctic, and 1993 Antarctic winters. The first column is an evolution of minimum temperatures T poleward of 40°N in the NH and of 40°S in the SH, the second column is latitudinal location of T_{min} as a function of time and the third and last columns show respectively the evolution of areas where $T < 197$°K and areas with $T < 187$°K. The shaded bars at the time axis indicate the periods when MLS and CLAES observed the polar regions of winters.

MLS, one at 90°E, another at 45°E, and the last at about 35°W. These are located at the vortex edges and correspond well to the simulated DHCl regions. On January 10 an area of high ClO concentrations is seen at about 40°W to 120°E, and between 50°–70°N. This region corresponds reasonably well to the DHCl distribution on that date.

To further examine the UARS measurements related to heterogeneous chemistry on PSCs during this NH winter, we look at the evolution of HNO_3, $ClONO_2$, and aerosol extinctions measured by CLAES; the distribution of HCl observed by HALOE; and the structure of H_2O from MLS. Plate 2 shows CLAES observations of $ClONO_2$, HNO_3, and aerosol extinc-

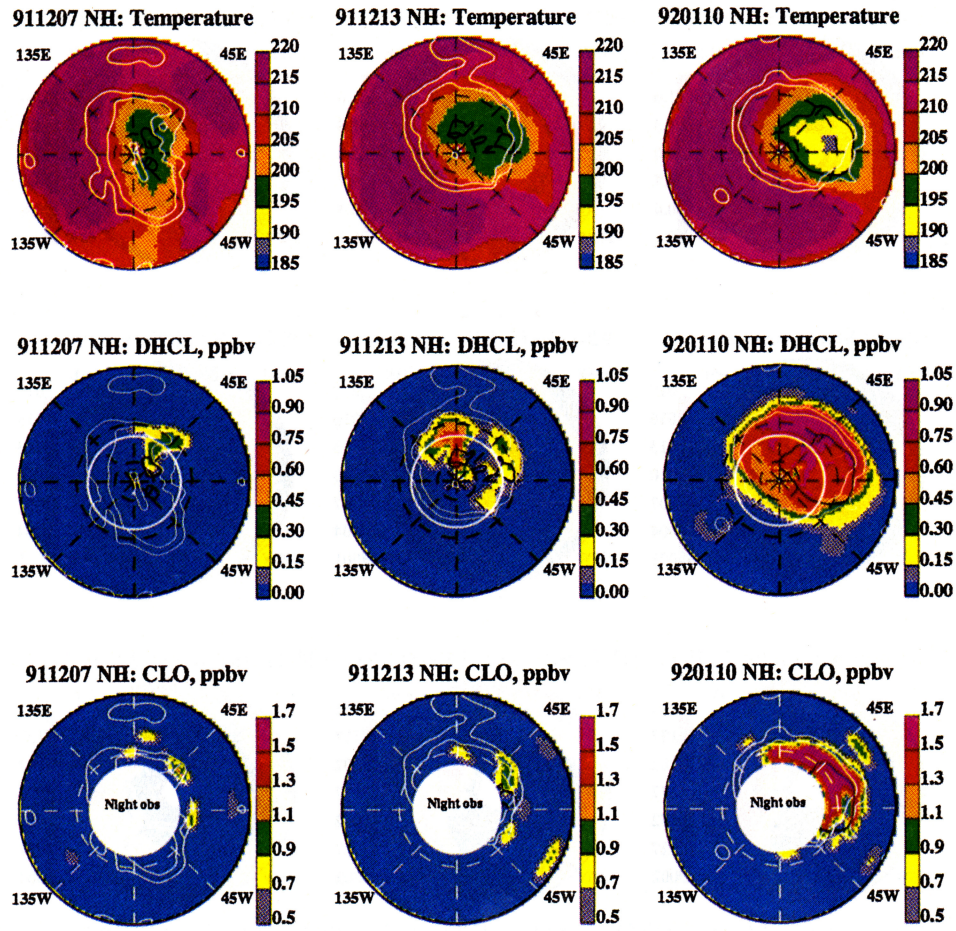

Plate 1. GEOS-DAS maps of (top) temperature distributions, (middle) modeled DHCl maps on the 465°K isentropic surface, and (bottom) MLS maps of lower stratospheric ClO at 46 hPa for selected days during the 1991–1992 NH winter. ClO mixing ratios greater than 0.5 ppbv are shown. The outer latitudinal circle is 30°N, and the inner circles are 60°N and 80°N. The black contours indicate areas where $T < 197$°K, when they exist. The solid contours are PV values of 2.8×10^{-5} °K m^2 s^{-1} kg^{-1} (outer contour) and 2.5×10^{-5} °K m^2 s^{-1} kg^{-1} (inner contour) which indicate the approximate edge of the vortex. The Greenwich meridian lies along the horizontal line directed to the right.

tion on January 9, 10, and 11. We see low concentrations of $ClONO_2$ almost to 0.4 ppbv coincident with and downstream of the cold areas, as shown by the GEOS-DAS wind distribution (a white dashed line designates these areas), and relatively slight decreases of HNO_3 in the gas phase inside the cold areas where PSCs I and II are expected to occur. During January 9–11 the PSCs (as indicated by CLAES extinction measurements) are located close to the vortex edge, where large amounts of polar vortex air should circulate through these regions of polar processing. MLS did not observe significant dehydration of the Arctic lower stratosphere during this period. Both PSCs and the enhancement in the sulfate aerosols from the Mount Pinatubo eruption are thought to be important for polar chlorine activation [*Hanson et al.*, 1994; *Lefevre et al.*, 1994]. *Taylor et al.* [1994] and *Massie et al.* [1994] have shown that the different spectral properties of PSCs and sulfate aerosols can be used for their identification. Here we will use the spectral aerosol measure M, developed by *Massie et al.* [1994], and the processed CLAES aerosol extinction data for 925, 1257, and 1606 cm^{-1} [*Roche et al.*, 1994] for this purpose. The predicted aerosol measure M values for the PSCs and sulfate aerosols, as a function of temperature, fall into distinct groups [e.g., *Massie et al.*, 1994, Figures 3 and 14]. The positive M values between 0.7 and 1.2 for PSC particles have been theoretically and observationally associated with temperatures less than 200°K. Theoretical calculations imply that sulfate particles have negative values of M. Depending on the H_2SO_4 concentrations, M varies from -0.5 to -2.5, and these negative M values are found in the temperature range 210°–235°K. *Massie et al.* [1994] discussed the behavior of the M values on August 18, 1992, in the SH to illustrate the spectral signature of sulfate aerosols, PSCs, and particles of intermediate composition at 46 hPa. They showed that multiwavelength aerosol extinction observations can be used to determine the locations of sulfate and PSC particles. Changes of M between middle and high latitudes are consistent with theoretical aerosol spectra for sulfate and PSC particles, and the M values associated with the NAT particles in the polar region are located in cold areas where the temperatures drop below the NAT temperature threshold. The calculated M values for January 10, 1992, are plotted in Plate 3a to illustrate the consistency of the appearance of PSC signatures with regions of cold air at 46 hPa. The green triangles with $M < -0.91$ correspond to sulfate aerosols. The blue squares ($-0.91 < M < +0.26$)

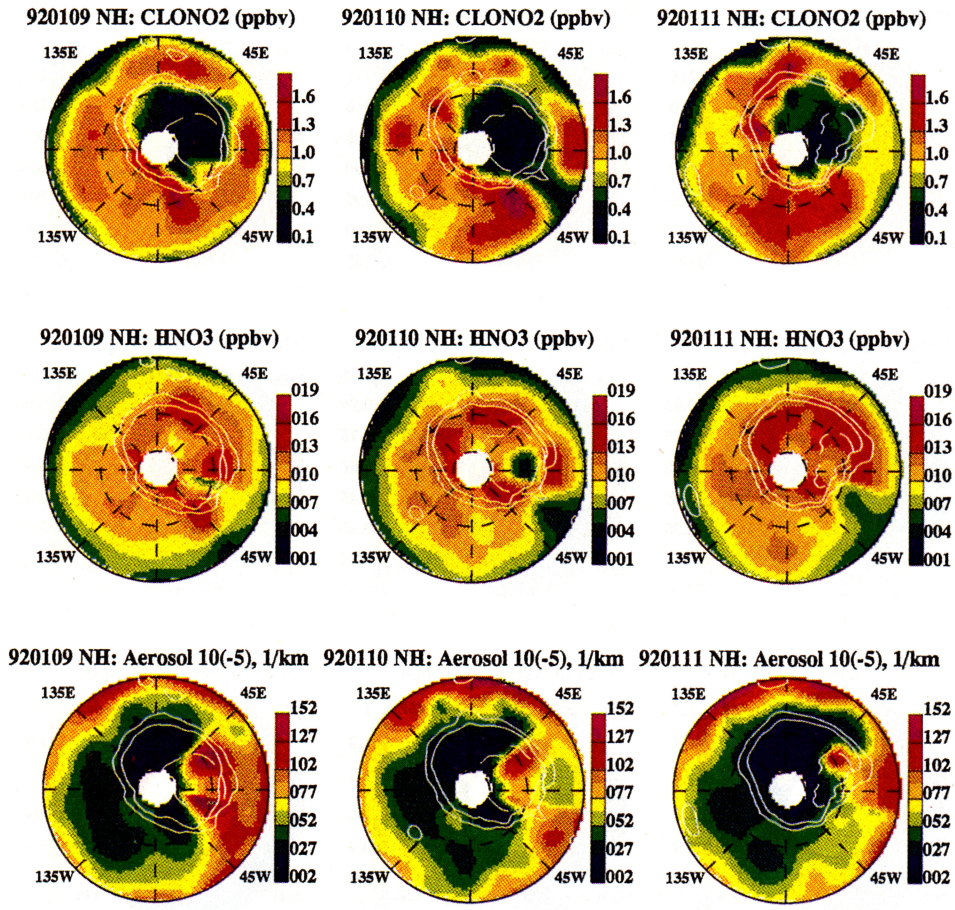

Plate 2. CLAES maps of (top) $ClONO_2$, (middle) HNO_3, and (bottom) aerosol extinction coefficients at 46 hPa in the NH during January 9–11, 1992. Polar projection and contours are the same as in Plate 1.

correspond to particles of intermediate composition, and the red crosses with ($M > 0.26$) represent PSC particles. We see that most of the sulfate particles lie in regions where $T >$ 205°K (outside the polar vortex) while PSC particles are in regions where $T < 205$°K (inside the vortex), and particles of intermediate composition occur over a rather broad temperature region. Red crosses, reflecting approximately "pure" PSCs, are in the regions of coldest temperatures ($T < 197$°K), where maximum aerosol extinctions exist, as do decreases of HNO_3 and depletions of $ClONO_2$ (Plates 1 and 2). Plate 3b illustrates the variability of the NAT threshold temperatures graphed as a function of HNO_3 (green diamonds) and H_2O (red triangles) measured by CLAES in the region between 46° and 54°N. We see that the changes in the measured VMRs of HNO_3 and H_2O on January 10, 1992, lead to the NAT temperature variations with amplitude 2.5°K around the commonly used threshold value of 195°K in the lower stratosphere. The consistency of the predicted heterogeneous depletion of HCl with the longitudinal structures of the aerosol composition, CLAES temperature, and HALOE HCl are illustrated by Plates 3c and 3d at 46 hPa in the latitudinal range 46°–54°N (except for the HALOE measurements of HCl, which are in the range 47°–48°N). We see that outside of the polar vortex the measured HCl VMRs are about 0.8–1.1 ppbv, while the average modeled level for the HCl VMRs is a bit less. Despite such quantitative disagreement (which is probably due to the simplicity of our modeling procedure), the shape of the modeled longitudinal structure of HCl with and without the influence of heterogeneous reaction (1) confirms the agreement between the location of polar-processed air and the measured depletion of HCl near the vortex edge, where locations of PSC particles (red triangles of M) are observed. The temperatures ($T < T_c$ around 0°E where PSCs are expected) also correspond well to the calculations of the positive values of aerosol measure M that are indicative of PSCs. Looking at the inner and boundary regions of the vortex (around 0°E) we see that inside the vortex the ClO VMRs reach about 1.5–1.8 ppbv while the ($ClONO_2$ + HCl) VMRs drop from about 2 ppbv outside the vortex to about 0.9 ppbv inside, as shown by the MLS, CLAES and HALOE measurements (Plates 1–3; see also *Geller et al.* [1995, Figure 2]). The HNO_3 VMRs on January 10 go down to about 4 ppbv where the CLAES temperature is less than 190°K (Plate 2).

The differences between the evolution of polar processing during the early stages of the first two Arctic and Antarctic winters of the UARS mission are illustrated by Figure 1. As is seen from the first row of Figure 1 for the winter of 1991–1992, PSC formation is possible from early December until January 22 with a further event on January 27 at 46 hPa. This corresponds well to the behavior of the minimum temperature in the European Center for Medium-Range Weather Forecasts (ECMWF) analyses as discussed by *Chipperfield* [1994]. In the winter of 1992–1993, the PSCs should have first formed during the end of November 1992, which is 1 week earlier than was the case in 1991. The PSCs, as in winter 1991–1992, occurred sporadically throughout December, and after January 2, polar

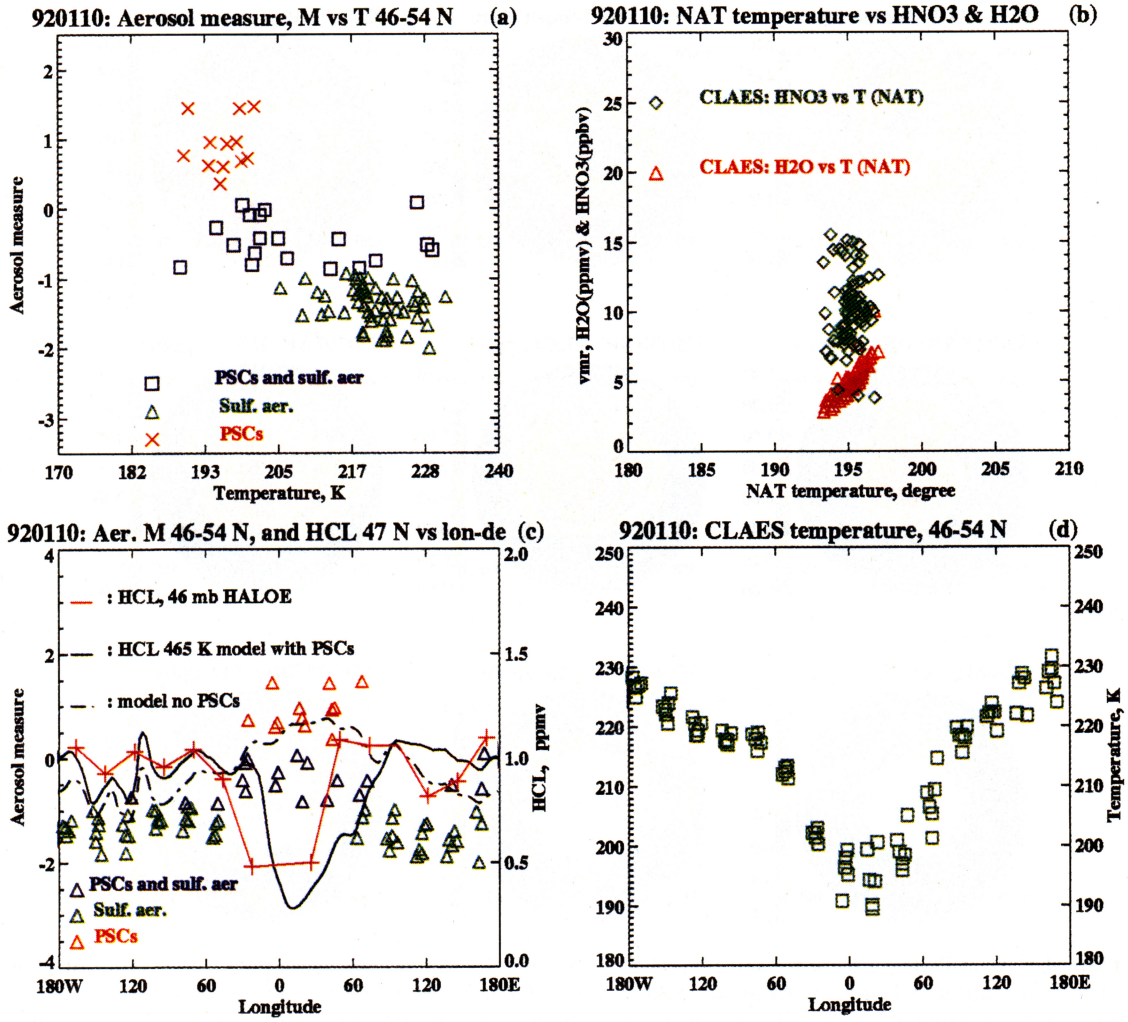

Plate 3. Features of polar processing at 46 hPa for the latitude range 46°–54°N as seen by CLAES, HALOE, and modeled DHCl on January 10, 1992. (a) Aerosol spectral measure M values, graphed as a function of CLAES temperature, (b) Variability of the NAT equilibrium temperature as a function of HNO_3 and H_2O volume-mixing ratios measured by CLAES for latitudes 46°–54°N. (c) M values as a function of latitude for the latitude range 46°–54°N, HALOE HCl VMR, and modeled HCl with and without heterogeneous losses at 47°N, (d) CLAES temperature as a function of longitude. All values are shown at 46 hPa.

processing should have occurred throughout the remainder of January. Note that during the first half of December 1991, the GEOS-DAS analyses show that the cold areas, where PSCs are expected, are larger than the cold areas during the first half of December 1992. During 1991–1992 the GEOS-DAS analyses shows that there were several times (around December 13 and 27 January 10 and 22) when the locations of the minimum temperature in the lower stratosphere at 46 hPa and/or above are shifted equatorward to 60°N. During 1992–1993, however, only at the beginning of December (when sporadic polar-processing events are observed) do the locations of the regions with minimum temperatures occur at latitudes down to 60°N. The PV also shows significant southward shifts of the vortex during the 1991–1992 winter, when the vortex was filled with chemically processed air. The main features of polar processing in the Arctic winter 1992–1993 have also been studied and compared with UARS data. From November 29, 1992, to January 8, 1993, when CLAES and MLS were monitoring the polar regions, the occurrences of polar-processing events as predicted by DHCl distributions from the transport model agree qualitatively with the observed structure of the high values of MLS ClO as well as with $ClONO_2$, HNO_3 decreases, and enhanced values of aerosol extinctions measured by CLAES in the cold areas of the polar vortex, where PSCs are expected. (See also *Waters et al.* [1995] for a description of the MLS ClO observations during the 1992–1993 NH winter.) The H_2O maps produced by MLS do not show any dehydration in the lower stratosphere during the early stages of the NH winter 1992–1993, as was also found by *Santee et al.* [1995].

5.2. Southern Hemisphere Winters 1992 and 1993

The third row of Figure 1 summarizes the GEOS-DAS picture of the minimum temperature evolution southward of 40°S in the south polar region from May 1 to July 31, 1992. The first polar-processing events at 46 hPa can be observed after May 8. The first occurrence of areas where temperatures are less than 187°K (cold enough for PSC II or ice particle formation) is seen in the GEOS-DAS analysis around June 10. Several days later, GEOS-DAS shows significant decrease in the areas which are cold enough for PSC II formation without any sig-

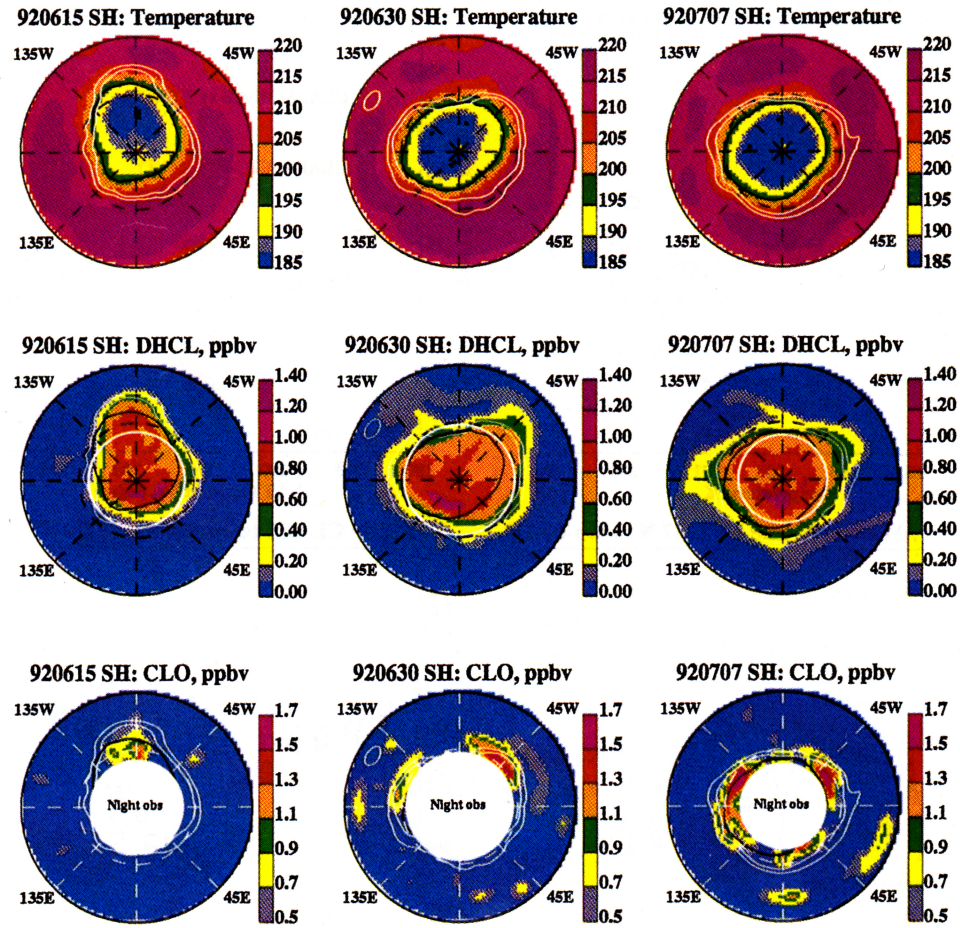

Plate 4. As in Plate 1 except for selected days of the 1992 SH winter. The south pole is the center of each map. Three latitudinal circles correspond to 30°S (outer), 60°S, and 80°S. White contours designate the vortex edges with PV values of -2.5×10^{-5} °K m^2 s^{-1} kg^{-1} (outer contour) and -2.8×10^{-5} °K m^2 s^{-1} kg^{-1} (inner contour).

nificant changes in the area where $T < 197$°K. After June 15 the extent of the cold area, where PSCs can exist, remains about constant. The areal extent with temperatures less than 197°K levels off near its maximum value by about July 1, and after that the coldest polar areas occupy approximately 50% of the southern areas poleward of 40°S. On reaching this maximum areal extent, however, the minimum temperatures continue to decrease after July 1. The temperature maps indicate that polar-processing events at relatively low polar latitudes occurred during May 9–13, around May 28, and during June 10–14, when the position of cold air shifts northward of 70°S at some longitudes. During the middle of June, when the GEOS-DAS analyses indicate a rapid decrease of the areal extent where $T < 187$°K, there should have been substantial PSC II evaporation.

Plate 4 shows SH GEOS-DAS temperatures, modeled DHCl, and MLS ClO maps for selected days during June and July 1992. MLS and CLAES were looking northward during May (Figure 1), and UARS experienced malfunctions during the period June 2–17 that caused reduced operations. Thus in Plate 5, maps of $ClONO_2$, HNO_3, and aerosol extinction measured by CLAES are plotted for only 3 selected days of June and July. The temperature maps in Plate 4 show that on June 15 the cold areas where $T < 195$°K (the 195°K isotherm is denoted by a black line) have occupied approximately two thirds of the polar vortex area and that a significant part of the coldest air mass is located in the western hemisphere. Areas where $T < 195$°K have spread out to latitudes lower than 60°S. On June 30, the cold air mass is oriented along the 25°W to 165°E line. In particular, a large part of the coldest air with $T < 190$°K lies above the line of 45°W to 135°E. On July 7 the configuration of the coldest air has became more circular with its center almost over the south pole. The boundaries of the fully developed polar processing in the SH, as defined by our DHCl calculations, were found to be given by the -2.8×10^{-5} and -2.5×10^{-5} PV unit contours on the 465°K isentropic surface. These contours are shown in white in Plate 4. From the DHCl calculations we found that polar processing began on May 9, at about 65°W, 75°S, close to the vortex edge. The region of high DHCl values has expanded considerably by May 13 and fills the vortex by May 25. After this the region of polar processing is determined by the undulations in the polar vortex as seen in the second row of Plate 4. The last row of Plate 4 represents MLS ClO observations on the 46-hPa surface. MLS also obtained a 24-hour period of Antarctic observations during June 1–2, 1995 (immediately before the UARS malfunction), and detected enhanced ClO in the sunlit vortex [*Waters et al.*, 1993b] as expected from the low-temperature distribution that occurred before this time. On June 15 a large region of enhanced ClO with VMR > 0.6 ppbv is seen extending from

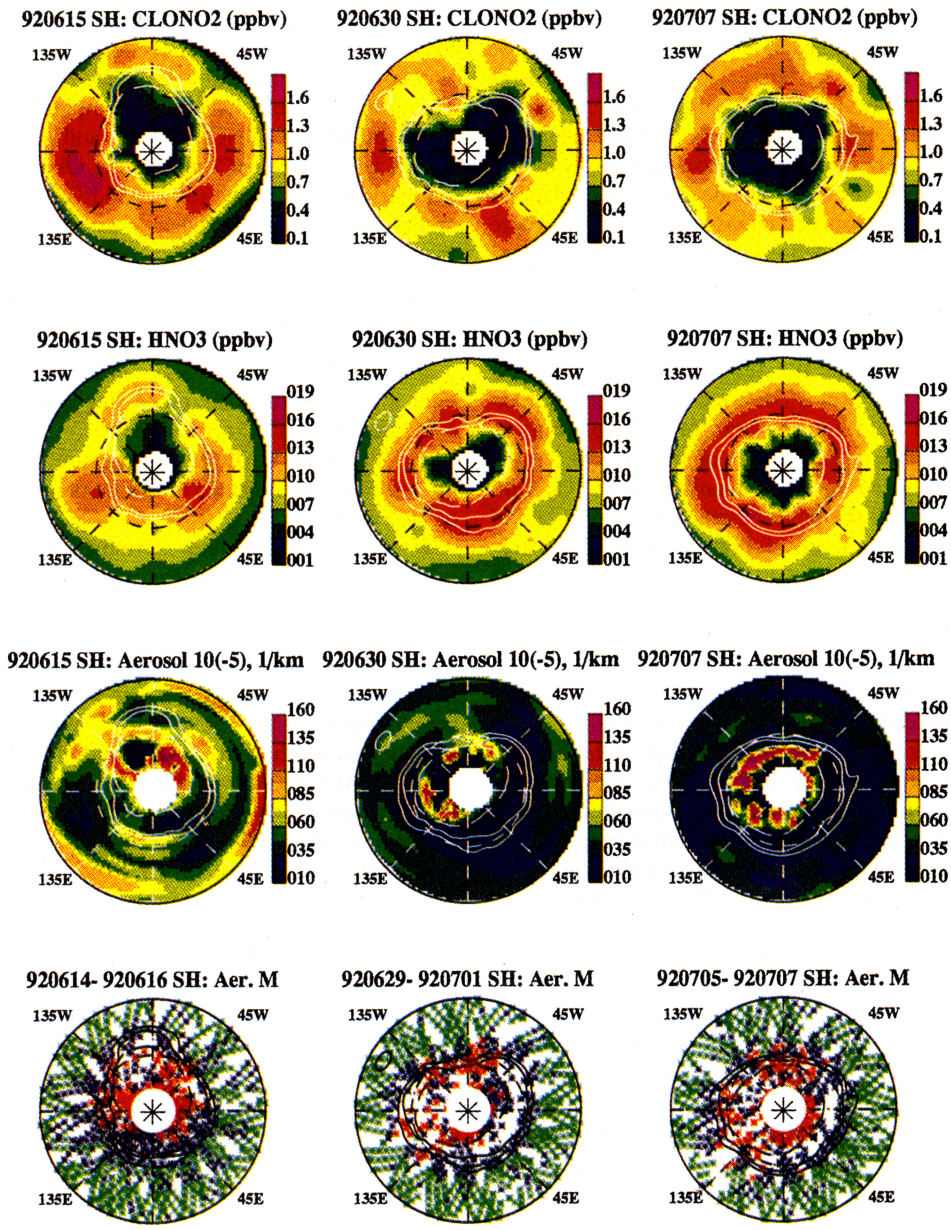

Plate 5. CLAES maps of $ClONO_2$ (first row) and HNO_3 (second row) and aerosol extinction coefficient (third row) for June 15, June 30 and July 7 during the 1992 SH winter. The PV and 195°K contours are shown in white. Last row shows the maps of the aerosol measure *M* during June 14–16, June 30 to July 1, and July 5–7. Red, blue, and green stars designate locations of PSC, PSC/sulfate mixtures, and sulfate particles. All maps are at 46 hPa.

85°W to 120°W between the latitudes 50°S and 65°S. This location is in good agreement with the DHCl for this day at the western vortex edge in sunlight. A comparison of the ClO maps with the sunlit DHCl distribution on June 30 also shows reasonable agreement in the sunlit parts of the western polar vortex. It is difficult to explain the occurrences of other weak patches of ClO outside the polar vortex. On July 7, MLS measurements show several patches of enhanced ClO VMR, but only the vortical belts of ClO are straightforwardly explained by the DHCl distributions around the vortex edge at 40°W, 90°W, 180°E, and 90°E. The others, located outside the vortex and centered at 25°E, 90°E, and 115°W, are likely due to MLS ClO measurements being noisier on this day because MLS spectral band 3, which provides measurements on the ClO spectral line wing, was off owing to UARS solar array drive problems.

To add to this picture given by our simple DHCl calculations and the observed ClO distributions we look at CLAES maps of $ClONO_2$, HNO_3, and aerosols (Plate 5) and compare them with the meteorological conditions and the DHCl and ClO maps (Plate 4). Inspection of the $ClONO_2$ maps from June 11 to July 7 (selected days are plotted in the first row of Plate 5) shows that $ClONO_2$ volume mixing ratios less than 0.4 ppbv are observed by CLAES inside the coldest areas of the vortex. The zones of relatively low concentrations of $ClONO_2$ with VMRs between 0.4 and 1.0 ppbv are surrounded by areas of CLAES temperatures in the interval between 200°K and 210°K and might be linked to heterogeneous reactions of $ClONO_2$

with HCl and/or H_2O on the surfaces of sulfate aerosols. Inspection of the aerosol measure M maps (bottom row) shows that inside and outside of the boundary of the polar vortex there were significant concentrations of sulfate particles (green stars) and PSC/sulfate mixtures (blue stars). Heterogeneous loss of $ClONO_2$ is likely on these surfaces in regions of low temperatures, especially in the volcanically perturbed polar regions of the lower stratosphere [*Hanson et al.*, 1994], where the effects vary strongly with latitude because of temperature, downward transport and HNO_3 variations. This is seen by the evolution of HNO_3 maps in the second row of Plate 5. HNO_3 decreases, with VMR < 7 ppbv, are observed by CLAES only in the coldest areas, where the temperature drops below 190°K; the existence of PSCs is confirmed by the aerosol extinction maps (third row) and the aerosol M maps (bottom row). During the beginning and middle of June, CLAES maps of HNO_3 show localized regions of enhanced HNO_3 with VMR > 13 ppbv around the polar vortex edge. By the end of June and during the first week of July, however, the vortex edge is surrounded by a belt of high values of HNO_3, with VMR > 13 ppbv. The aerosol extinction maps in the 790, 925, 1265, and 1605 cm^{-1} channels show significant changes in the optical absorption attributable to the transport of the "pure" sulfate clouds. Looking at the aerosol maps, we find a decrease of the sulfate cloud extinction outside the vortex edges, while inside the vortex, areas of high aerosol extinctions are enhanced, and polar processing on PSCs and particles of intermediate composition has developed (as indicated by the $ClONO_2$ maps). The intense diabatic descent during this period is probably the main reason for the behavior of the HNO_3 and aerosols at and outside the vortex edge. The influence of the diabatic downward transport of air on the distribution of long-lived species was clearly shown by the time evolution of vertical profiles of N_2O and CH_4 measured by CLAES [*Roche et al.*, 1993, 1994; *Kumer et al.*, 1993]. Our inspection of altitude changes in the CLAES N_2O VMR contours between June 11 and July 7 also confirms that strong downward transport is occurring.

The bottom row of Figure 1 summarizes the minimum temperature evolution south of 40°S in the south polar region from May 1 to July 31, 1993 according to GEOS-DAS. We see that the first intense polar processing events in the lower stratosphere occurred after May 10, when the cold areas at 46 hPa were spreading out over 10–20% of the south polar region. The first occurrence of areas where temperatures were less than 187°K, according to GEOS-DAS analyses, was around June 1, 10 days earlier than in the SH winter 1992. During June 1993, GEOS-DAS analyses do not show significant changes in the minimum temperatures, although the areas where PSC I are expected to occur increases from 30% to 40%. After July 1 the cold areas, where PSC I and II might exist, occupy approximately 50% of areas polarward of 40°S. The geographical distributions of most of the polar-processing events as indicated by the DHCl maps agree quite well with the MLS maps of ClO in the sunlit areas of the SH lower stratospheric polar vortex during the early stages of the 1993 SH winter from May 28 to July 7.

6. Summary and Conclusions

Results from an off-line transport model for diagnostics of polar processing events have been shown for the early parts of the first two NH and SH winters observed by UARS. This transport model is formulated assuming PSC formation at low temperatures with subsequent conversion of the reservoir chlorine species $ClONO_2$ and HCl into active chlorine radicals. These model results have been compared with ClO measurements by MLS; $ClONO_2$, HNO_3, and aerosol measurements from CLAES; and HCl measurements from HALOE. These comparisons generally show good agreement between the model calculations and what is expected from the generally accepted paradigm for polar processing of chlorine species on PSCs. In particular, the following are seen:

1. Enhanced ClO VMRs, measured by MLS, are seen where the modeled polar processed air is in sunlight.
2. CLAES measured low concentrations of $ClONO_2$ are seen in regions of polar processing where temperatures are cold enough for PSC formation.
3. Where the HALOE measurement track intersects polar-processed air, as indicated by our modeling, low concentrations of HCl are seen.
4. The spectral signatures from CLAES observations show sulfate aerosols at all latitudes and under all temperature conditions both outside (major part) and inside (~ much smaller fraction) the polar vortex. PSC particles are seen where cold temperatures occur inside the polar vortex, and particles of intermediate composition are seen both inside and just outside the boundary of the polar vortex, where temperatures are slightly warmer than the NAT threshold values.
5. CLAES measurements of HNO_3 show decreases where temperatures are very cold, especially under Antarctic winter conditions, when PSC II formation is expected. Small decreases of HNO_3 are seen by CLAES during the Arctic winters.

In comparing early winter polar processing for the two hemispheres as well as during different years, we see that in the NH a period of sporadic polar processing initially takes place (as illustrated by *Douglass et al.* [1993]) before a "permanent" region of polar processing becomes established. As the air flows through this polar-processing region, chemically processed air fills the vortex. After this time, undulations in the polar vortex define the region of processed air. In the SH, polar processing, once begun, steadily proceeds to fill the vortex. The filling of the vortex in both hemispheres takes a bit over 2 weeks from the beginning of polar processing in the SH and from the establishment of a region of "permanent" polar processing in the NH. Little interannual variability is seen in the time sequencing of polar processing in early winter in either the NH or SH for the years examined here. Our modeling results for the evolution of polar processing during the first part of January 1992 and 1993 together with UARS measurements indicate the very strong dependence of the location of the polar-processed air on meteorological conditions. In particular, a shift of the vortex to midlatitudes during January 1992 and the occurrence of PSCs around the north pole during January 1993 was seen (see also *Chipperfield* [1994]). The diagnostic results of *Chipperfield* [1994] for polar processing during the entire Arctic winters of 1991–1992 and 1992–1993 and trajectory analyses of motion in the polar region for NH and SH winters 1992–1994 by *Manney et al.* [1994] have shown much more interannual variability in the later winter progression of events in the lower stratosphere.

The generally good qualitative agreement between our off-line polar processing transport model and UARS measurements gives increased confidence that the initiation of the polar processing of chlorine reservoir species to reactive species on NAT particles that form in cold regions is qualitatively

well understood. It illustrates the capabilities of our simple polar processing model, as well as more complex chemistry-transport models, to provide valuable information on the evolution of the polar lower stratosphere during early winter periods when UARS measurements are fragmentary as a result of orbital and viewing limitations. It is interesting to note that although the planning and instrument selection for UARS took place before the discovery of the Antarctic ozone hole and the realization of the importance of polar heterogeneous chemistry, the UARS measurements have proven very valuable in validating many important aspects of polar stratospheric chemistry.

Acknowledgments. The authors wish to thank S. Massie and S. P. Smyshlyaev for useful comments and discussions. This research was supported by the Upper Atmosphere Research Satellite project under NASA contract NAG-53177.

References

Allen, D. J., A. R. Douglass, R. B. Rood, and P. D. Guthrie, Application of monotonic upstream-biased transport scheme to the three-dimensional constituent transport calculations, *Mon. Weather Rev.*, *119*, 2456–2464, 1991.

Barath, F., et al., The Upper Atmosphere Research Satellite microwave limb sounder instrument, *J. Geophys. Res.*, *98*, 10,751–10,762, 1993.

Cerniglia, M. C., R. B. Rood, and A. R. Douglass, Three-dimensional simulation of the influence of a cutoff low on the distribution of northern hemisphere processed air in late January 1992, *J. Geophys. Res.*, *100*, 16,431–16,433, 1995.

Chipperfield, M. P., A three-dimensional model comparison of PSC processing during the Arctic winters of 1991/92 and 1992/1993, *Ann. Geophys.*, *12*, 342–354, 1994.

Chipperfield, M. P., D. Cariolle, and P. Simon, A three-dimensional transport model study of PSC processing during EASOE, *Geophys. Res. Lett.*, *21*, 1463–1466, 1994.

Danilin, M. Y., and J. C. McConnell, Heterogeneous reactions in a stratospheric box model: A sensitivity study, *J. Geophys. Res.*, *99*, 25,681–25,696, 1994.

Douglass, A. R., R. B. Rood, J. A. Kaye, R. S. Stolarski, D. J. Allen, and E. M. Larson, The influence of polar heterogeneous processes on reactive chlorine at middle latitudes: Three-dimensional model implications, *Geophys. Res. Lett.*, *18*, 25–28, 1991.

Douglass, A. R., R. B. Rood, J. Waters, L. Froidevaux, W. Read, L. Elson, M. Geller, Y. Chi, M. Cerniglia, and S. Steenrod, A 3D simulation of the early winter distribution of reactive chlorine in the north polar vortex, *Geophys. Res. Lett.*, *20*, 1271–1274, 1993.

Elson, L. S., and L. Froidevaux, Use of Fourier transforms for asynoptic mapping: Application to the Upper Atmosphere Research Satellite microwave limb sounder, *J. Geophys. Res.*, *98*, 23,039–23,049, 1993.

Farman, J. C., B. G. Gardiner, and J. D. Shanklin, Large losses of total ozone in Antarctica reveal seasonal ClO_x/NO_x interaction, *Nature*, *315*, 207–210, 1985.

Geller, M. A., Y. Chi, R. B. Rood, A. R. Douglass, D. J. Allen, M. Cerniglia, and J. W. Waters, 3-D transport chemistry studies of the stratosphere using satellite data together with data assimilation, in *Impact of the Stratosphere on Climate and Biosphere*, edited by M. L. Chanin, pp. 179–198, Kluwer Acad., Norwell, Mass., 1993.

Geller, M. A., V. A. Yudin, A. R. Douglass, J. W. Waters, L. S. Elson, A. E. Roche, and J. M. Russell III, UARS measurements verification of the polar processing paradigm, *Geophys. Res. Lett.*, *22*, 2937–2940, 1995.

Hanson, D., and K. Mauersberger, Laboratory studies of the nitric acid trihydrate: Implications for the south polar stratosphere, *Geophys. Res. Lett.*, *15*, 855–859, 1988.

Hanson, D., A. R. Ravishankara, and S. Solomon, Heterogeneous reactions in sulfuric acid aerosols: A framework for model calculations, *J. Geophys. Res.*, *99*, 3615–3629, 1994.

Kaye, J. A., A. R. Douglass, R. B. Rood, R. S. Stolarski, P. A. Newman, D. J. Allen, and E. M. Larson, Spatial and temporal variability of the extent of chemically processed stratospheric air, *Geophys. Res. Lett.*, *18*, 29–32, 1991.

Kumer, J. B., J. L. Mergenthaler, and A. E. Roche, CLAES CH_4, N_2O and CF_2CL_2(F 12) global data, *Geophys. Res. Lett.*, *20*, 1239–1242, 1993.

Lary, D. J., W. A. Norton, M. P. Chipperfield, J. A. Pyle, and L. P. Riishojgaard, An equivalent PV latitude-potential temperature viewpoint of the atmosphere applied to general diagnostics and tracer intialisation, *Q. J. R. Meteorol. Soc.*, *121*, 187–210, 1995.

Lefevre, F., G. P. Brasseur, I. Folkins, A. K. Smith, and P. Simon, Chemistry of the 1991–1992 stratospheric winter: Three-dimensional model simulations, *J. Geophys. Res.*, *99*, 8183–8195, 1994.

Manney, G. L., R. W. Zurek, A. O. Neil, and R. Swinbank, On the motion of air through the stratospheric polar vortex, *J. Atmos. Sci.*, *51*, 2973–2994, 1994.

Massie, S. T., P. L. Bailey, J. C. Gilley, E. C. Lee, J. L. Mergenthaler, A. E. Roche, J. B. Kumer, E. F. Fishbein, J. W. Waters, and W. A. Lahoz, Spectral signatures of polar stratospheric clouds and sulfate aerosol, *J. Atmos. Sci.*, *51*, 3027–3044, 1994.

Murphy, D. M., and A. R. Ravishankara, Temperature averages and rates of stratospheric reactions, *Geophys. Res. Lett.*, *21*, 2471–2474, 1994.

Reber, C. A., The Upper Atmosphere Research Satellite, *Geophys. Res. Lett.*, *20*, 1215–1218, 1993.

Roche, A. E., J. B. Kumer, J. L. Mergenthaler, G. A. Ely, W. G. Uplinger, J. F. Potter, T. C. James, and L. W. Sterritt, The cryogenic limb array etalon spectrometer (CLAES) on UARS: Experiment description and performance, *J. Geophys. Res.*, *98*, 10,763–10,775, 1993a.

Roche, A. E., J. B. Kumer, and J. L. Mergenthaler, CLAES observations of $ClONO_2$ and HNO_3 in the Antarctic stratosphere between June 15, and September 17, 1992, *Geophys. Res. Lett.*, *20*, 1223–1226, 1993b.

Roche, A. E., J. B. Kumer, J. L. Mergenthaler, R. W. Nightingale, W. C. Uplinger, G. A. Ely, J. F. Potter, D. J. Wuebbles, P. S. Connel, and D. E. Kinnsison, Observations of lower-stratospheric $ClONO_2$, HNO_3, and aerosol by the UARS CLAES experiment between January 1992 and April 1993, *J. Atmos. Sci.*, *51*, 2877–2902, 1994.

Rodriguez, J. M., M. K. Ko, and N. D. Sze, Role of heterogeneous conversion of N_2O_5 on sulfate aerosols in global ozone losses, *Nature*, *352*, 134–137, 1991.

Russell, J. M. III, L. L. Gordley, J. H. Park, S. R. Drayson, A. F. Tuck, J. E. Harries, R. J. Cicerone, P. J. Crutzen, and J. E. Frederick, The Halogen Occultation Experiment, *J. Geophys. Res.*, *98*, 10,777–10,797, 1993.

Santee, M. L., W. G. Read, J. W. Waters, L. Froidevaux, G. L. Manney, D. A. Flower, R. F. Jarnot, R. S. Harwood, and G. E. Peckerman, Interhemispheric differences in polar stratospheric HNO_3, H_2O, ClO and O_3, *Science*, *267*, 849–852, 1995.

Schoeberl, M. R., et al., The evolution of ClO and NO along air parcel trajectories, *Geophys. Res. Lett.*, *20*, 2511–2514, 1993a.

Schoeberl, M. R., R. S. Stolarski, A. R. Douglass, P. A. Newman, L. R. Lait, J. W. Waters, L. Froidevaux, and W. G. Ready, MLS ClO observations and Arctic polar vortex temperatures, *Geophys. Res. Lett.*, *20*, 2861–2864, 1993b.

Schubert, S. D., R. B. Rood, and J. Pfaendtner, An assimilated dataset for Earth science applications, *Bull. Am. Meteorol. Soc.*, *74*, 2331–2342, 1993.

Smyshlyaev, S. P., and V. A. Yudin, Numerical simulation of ozone changes due to aircraft perturbations, *Izv. Russ. Acad. Sci. Atmos. Oceanic Phys.*, English Translation, *31*, 116–125, 1995.

Solomon, S., Progress toward a quantitative understanding of Antarctic ozone depletion, *Nature*, *347*, 347–354, 1990.

Taylor, F. W., A. Lambert, R. G. Grainger, C. D. Rodgers, and J. J. Remedios, Properties of northern hemisphere polar stratospheric clouds and volcanic aerosol in 1991/92 from UARS/ISAMS satellite measurements, *J. Atmos. Sci.*, *51*, 3019–3026, 1994.

Tuck, A. F., et al., Polar stratospheric cloud processed air and potential vorticity in the northern hemisphere lower stratosphere at midlatitudes during winter, *J. Geophys. Res.*, *97*, 7883–7904, 1992.

Toohey, D. W., L. M. Avallone, L. R. Lait, P. A. Newman, M. R. Schoeberl, D. W. Fahey, E. L. Woodbridge, and J. G. Anderson, The seasonal evolution of reactive chlorine in the northern hemisphere stratosphere, *Science*, *261*, 1134–1136, 1993.

Waters, J. W., L. Froidevaux, W. G. Read, G. L. Manney, L. S. Elson, D. A. Flower, R. F. Jarnot, and R. S. Harwood, Stratospheric ClO

and ozone from the microwave limb sounder on the Upper Atmosphere Research Satellite, *Nature*, *362*, 597–602, 1993a.

Waters, J. W., L. Froidevaux, W. G. Read, G. L. Manney, and L. S. Elson, MLS observations of lower stratospheric ClO and O_3 in the 1992 southern hemisphere winter, *Geophys. Res. Lett.*, *20*, 1219–1222, 1993b.

Waters, J. W., G. L. Manney, W. G. Read, L. Froidevaux, D. A. Flower, and R. F. Jarnot, UARS MLS observations of lower stratospheric ClO in the 1992–93 and 1993–94 Arctic winter vortices, *Geophys. Res. Lett.*, *22*, 823–826, 1995.

Waters, J. W., et al., Validation of UARS microwave limb sounder ClO measurements, *J. Geophys. Res.*, *101*, 10,091–10,127, 1996.

M. C. Cerniglia and A. R. Douglass, Laboratory for Atmospheres, Code 916, NASA Goddard Space Flight Center, Greenbelt, MD 20771.

L. S. Elson and J. W. Waters, Jet Propulsion Laboratory, California Institute of Technology, 4800 Oak Grove Drive, Pasadena, CA 91109-8099.

M. A. Geller, B. V. Khattatov, and V. A. Yudin, Institute for Terrestrial and Planetary Atmospheres, State University of New York at Stony Brook, Stony Brook, NY 11794-5500. (e-mail: vyudin@uars.sunysb.edu)

A. E. Roche, Department 91-20 252, Lockheed Palo Alto Research Laboratory, 3251 Hanover Street, Palo Alto, CA 94303.

J. M. Russell, Mail Stop 401B, NASA Langley Research Center, Hampton, VA 23681.

(Received March 27, 1996; revised December 1, 1996; accepted March 17, 1997.)